Neuron
NeuroResource

A Modular Gain-of-Function Approach to Generate Cortical Interneuron Subtypes from ES Cells

Edmund Au,[1,2] Tanzeel Ahmed,[1,2] Theofanis Karayannis,[1,2] Shiona Biswas,[3] Lin Gan,[3,4] and Gord Fishell[1,2,*]
[1]NYU Neuroscience Institute
[2]New York University School of Medicine
NYU Langone Medical Center, 522 First Avenue, New York, NY 10016, USA
[3]Flaum Eye Institute, University of Rochester, Rochester, NY 14642, USA
[4]College of Life and Environmental Sciences, Hangzhou Normal University, Hangzhou, Zhejiang 310036, China
*Correspondence: gordon.fishell@med.nyu.edu
http://dx.doi.org/10.1016/j.neuron.2013.09.022

SUMMARY

Whereas past work indicates that cortical interneurons (cINs) can be generically produced from stem cells, generating large numbers of specific subtypes of this population has remained elusive. This reflects an information gap in our understanding of the transcriptional programs required for different interneuron subtypes. Here, we have utilized the directed differentiation of stem cells into specific subpopulations of cortical interneurons as a means to identify some of these missing factors. To establish this approach, we utilized two factors known to be required for the generation of cINs, *Nkx2-1* and *Dlx2*. As predicted, their regulated transient expression greatly improved the differentiation efficiency and specificity over baseline. We extended upon this "cIN-primed" model in order to establish a modular system whereby a third transcription factor could be systematically introduced. Using this approach, we identified *Lmo3* and *Pou3f4* as genes that can augment the differentiation and/or subtype specificity of cINs in vitro.

INTRODUCTION

The mammalian cortex is comprised of two main classes of neurons: excitatory long-range projection neurons (pyramidal cells) and inhibitory "short axon cells" (cortical interneurons, cINs). Numerous lines of evidence suggest a role for interneurons in regulating cortical rhythmicity, spike timing, and signal refinement, all of which are necessary for proper cortical circuit function (Cardin et al., 2009; Fino and Yuste, 2011; Klausberger and Somogyi, 2008; Kvitsiani et al., 2013; Lapray et al., 2012). Indeed, a number of disorders, such as schizophrenia, autism, bipolar disorder, and epilepsy, have cIN dysfunction and misregulation implicated as the possible underlying etiology (Belforte et al., 2010; Chao et al., 2010; Curley and Lewis, 2012; Fazzari et al., 2010; Konradi et al., 2011; Wang et al., 2011). Their involvement in various brain activities and disease states is not altogether surprising when one considers that as a group cINs are highly heterogeneous by a number of measures, including morphology, marker expression, and intrinsic electrophysiology, which themselves are a reflection of the diverse ways that they can impact neural function (Ascoli et al., 2008; Kawaguchi and Kondo, 2002). Therefore, given their importance, it would be of considerable value to be able to generate specific subclasses of cINs from stem cells in large numbers. This is an inherently difficult task, however, because the means by which different subtypes of cINs are developmentally specified is still only poorly understood.

Current methods for identifying cIN genes employ expression databases and bioinformatic screens as well as mouse genetic loss-of-function studies. With the former, a long list of candidate genes is produced, with only limited means to identify which merit follow-up analysis. The latter involves using mouse genetics, which is costly, time-consuming, and cannot detect genes with functional redundancy. To complement these existing approaches, we therefore wished to establish an ES cell-based gain-of-function (GOF) model system whereby transcription factors expressed early in cIN development can be systematically screened in vitro and subsequently transplanted in utero to assess their impact on cIN differentiation and subtype fate. We anticipated that this method would expand the capacity to efficiently screen through a large number of candidate genes, while also establishing functional criteria for identifying candidates that enable the production of pure populations of cIN subtypes and/or warrant further examination by mouse genetics.

Recent work has demonstrated that the differentiation of ES cells can be precisely directed to produce specific cell types within the nervous system, including spinal cord motor neurons, hypothalamic neurons, and cortical pyramidal cells (Eiraku et al., 2008; Gaspard et al., 2008; Wataya et al., 2008; Wichterle et al., 2001). For instance, it has recently been demonstrated that ES cell-generated pyramidal cells expressed proper layer markers and projection patterns and are produced in the correct temporal sequence. In fact, they were produced with specific enough fidelity that they integrated and established appropriate afferent connectivity upon transplantation (Eiraku et al., 2008; Gaspard et al., 2008). Similar efforts to produce cINs in large numbers and at high purity have proven problematic with current differentiation protocols (Maroof et al., 2010), although improvements

have recently been described (Maroof et al., 2013; Nicholas et al., 2013).

In an effort to boost differentiation efficiency, several groups have employed transcription factors to help guide ES-derived neural stem cells as well as somatic cells, such as fibroblasts, along signaling cascades normally used in development. This approach has been effective for generating midbrain dopaminergic neurons (Andersson et al., 2006; Martinat et al., 2006; Panman et al., 2011) and more recently in generating motor neurons (Lee et al., 2012; Mazzoni et al., 2013; Son et al., 2011). Building on these approaches, we sought to combine current genetic insights regarding intrinsic and extrinsic factors utilized in vivo for the generation of cINs and complement this with a forward genetic candidate approach.

We began this effort by determining if combinations of key factors known to be important in cIN development could be leveraged in a similar manner to transcriptionally specify ES cells to cINs of specific subclasses. Nkx2.1 has been shown to be critical for directing cIN identity and, upon exiting the cell cycle, for the selection of cIN subtype (Sussell et al., 1999; Butt et al., 2008; Nóbrega-Pereira et al., 2008). Either constitutive or conditional removal of *Nkx2-1* from the MGE results in a transfating of cortical interneurons produced from this structure to a CGE identity. In addition, members of the *Dlx* family of genes (*Dlx1*, *2*, *5*, and *6)* are present in the subpallium and are well recognized to be required for both cIN migration and more generally GABAergic neuronal fate (Anderson et al., 1997; Cobos et al., 2007; Stühmer et al., 2002a). Therefore, these two genes clearly play critical roles in both identity and positioning.

We therefore transcriptionally reprogrammed ES cells by sequential expression of Nkx2-1 followed by Dlx2, in a manner closely recapitulating that observed in vivo. Consistent with their prominent in vivo roles in the generation of cINs, we find that the efficiency of directing ES cell differentiation into cINs can be greatly enhanced. We then used this cIN-primed ES cell system to screen candidate transcription factors selected on the basis of being expressed in cIN progenitor zones but of unknown function. In total, 12 genes were tested in vitro. Of these, both LMO3 and Pou3f4 facilitated the differentiation of cINs. Whereas Pou3f4 greatly improved the efficiency of ES cell cIN differentiation in general, LMO3 augmented the differentiation of the MGE-derived basket cell population. Importantly, this result reliably predicted the phenotype of the LMO3 null mouse, which subsequent analysis revealed to have diminished basket interneuron numbers.

RESULTS

ES Cell-Derived Cortical Interneurons Exhibit Properties of In Vivo cINs

Cortical interneuron progenitors engrafted in utero into their site of origin exhibit a specialized migratory behavior into the neocortex (Butt et al., 2005; Nery et al., 2002; Wichterle et al., 2001). As a functional assay of cIN fate, we therefore began by testing whether neural progenitors derived from ES cells were capable of similar migration. Neural stem cells, differentiated at 90% efficiency as determined by *Sox1*-eGFP ES reporter line (gift from A. Smith, University of Cambridge) (Ying et al., 2003), were transplanted into MGE in utero, but despite successful transplantation (cells could be identified at the transplant site at postnatal day 21), none were ever found in the neocortex or hippocampus (Figure S1 available online). We therefore conclude that without further differentiation, neural stem cells per se do not efficiently become cortical interneurons. It also indicates that our in vivo transplantation approach provides a stringent test for the production of bona fide ES-derived cortical interneurons.

In their work, Watanabe et al. (2005) have demonstrated that mouse ES cells can be directed toward a telencephalic progenitor fate through early suppression of Wnt signaling. Moreover, as suggested by previous work on spinal cord (Wichterle et al., 2002), these cells become ventralized in the presence of sonic hedgehog (Shh) to give rise to subpallial progenitor populations (Watanabe et al., 2005). This work provided compelling in vitro evidence for ES-derived ventralized telencephalic progenitors being capable of becoming cINs. To test the fidelity of these cells to give rise to cINs, we transplanted them in utero and examined their fate postnatally. As a means to track the cells, we generated a pan-eGFP-expressing ES cell line by recombining out the stop cassettes from the RCE dual ES cell line, used previously to generate the RCE dual reporter mouse (hereafter referred to as the RCE line) (Miyoshi et al., 2010; Sousa et al., 2009). RCE ES cells were differentiated as previously described (Watanabe et al., 2005) to generate ventral telencephalic progenitors (Figures 1A–1C), a large proportion of which (approximately 50%) differentiated into GABAergic neurons (Figure 1D). At 11 days postdifferentiation, RCE embryoid bodies (EBs) were dissociated and transplanted into the MGE of e13.5 host embryos by UBM (Figure 1E). Three days after transplantation, the ventral injection site contained eGFP+ cells, from which unipolar and multipolar cINs were observed migrating dorsally into the host cortex (Figures 1F, 1F′, and 1F″). When analyzed postnatally, ES-derived cINs were observed in the cortex and expressed GABA (Figure 1G) as well as cIN subtype markers, including parvalbumin (indicative of MGE-derived cINs) and reelin (indicative of CGE-derived cINs) (Figures 1H and 1I). Although this provided proof of principle that cortical interneurons can be derived from ES cells in vitro, the efficiency of the transplanted cells to migrate to the cortex and assume cIN identity was extremely low (less than 1%).

Establishing an ES Cell Reporter Line for Cortical Interneuron Differentiation

Using these previously established methods as a starting point, it is clear that, contrary to unspecified neural stem cells, at least a small proportion can be differentiated into cortical interneuron progenitors by exposure to appropriate extrinsic signaling factors—progenitors that demonstrate appropriate migratory behavior and exhibit mature cIN phenotypes. However, when compared with MGE transplants, the efficiency of successfully engrafted cINs was found to be at best marginal. To improve upon these baseline conditions, we first generated a transgenic reporter ES cell line in order to readily gauge successful differentiation (Figure S2). This was accomplished by using the *Dlx5/6* intergenic element to drive eGFP expression (Stenman et al., 2003; Zerucha et al., 2000). In vivo, the *Dlx5*- and *Dlx6*-expressing

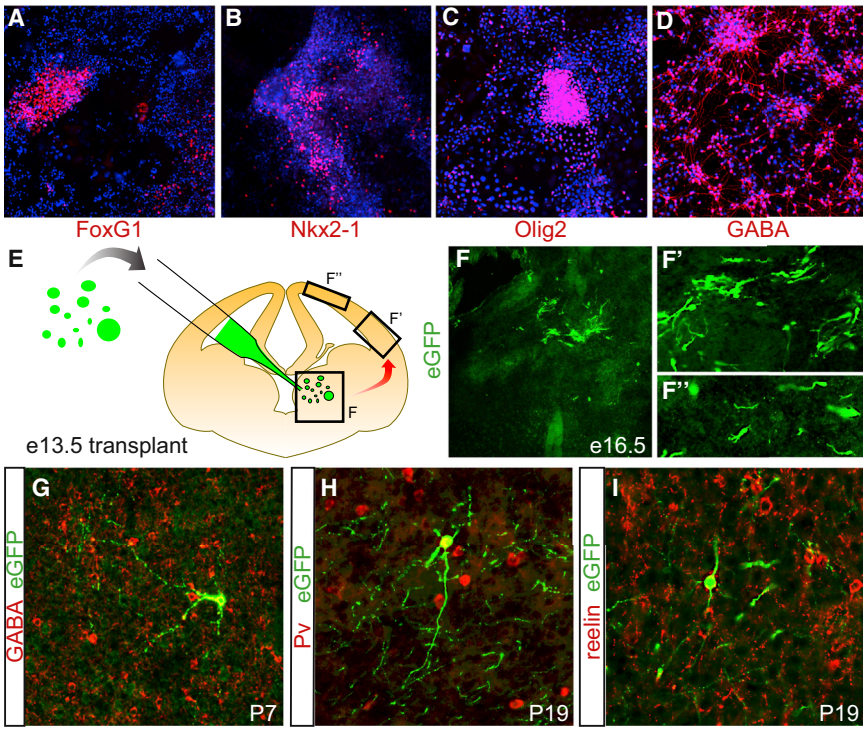

Figure 1. Exogenously Specified ES Cells Become Ventral Telencephalic Neural Precursors Capable of Long-Range Tangential Migration and Differentiation into Cortical Interneurons

(A–C) Embryoid bodies grown as adherent cultures express FoxG1 (A), Nkx2-1 (B), and Olig2 (C) after 9 days of differentiation.

(D) Upon dissociation, a large proportion of neurons are GABA positive.

(E and F) Schematic of transplantation strategy: a pan-eGFP-expressing line was differentiated for 11 days and then dissociated and transplanted into MGE of wild-type e13.5 Swiss Webster embryos (E). Three days following transplantation (e16.5), eGFP+ unipolar migratory cells were observed migrating away from the transplant site (F) and into the cortex (F′ and F″).

(G–I) Other transplant recipients were analyzed at P7 (G) and were GABA positive, and others were analyzed at P19 and coexpressed eGFP and cortical interneuron subtype markers, parvalbumin (PV) (H), and reelin (I).

See also Figure S1.

neuronal lineages encompass the entire neuronal output of the ventral telencephalon, including all cortical interneurons (Stühmer et al., 2002b; Zerucha et al., 2000), as well as a small population of dopaminergic projection neurons of the diencephalon (Andrews et al., 2003). As a means of verifying reporter fidelity, we generated multiple clonal lines that were then blastocyst injected. At e16.5, founder analysis was performed to identify clones with appropriate and robust eGFP expression that strongly resembled wild-type Dlx5/6-expression (Figures S1A–S1E). Having identified a reliable reporter, we differentiated the reporter ES cell line (referred hereafter as *Dlx5/6*-eGFP) and dissociated the resultant EBs to generate a neuronal monolayer. Consistent with our previous transplantation results, which indicated that only a small proportion of transplanted cells migrated dorsally to become cINs, eGFP was expressed in only a very small percentage of neurons differentiated in vitro (Figure S2F).

Transcriptional Specification of ES Cells

Extrinsic factors have been used extensively to guide ES cell differentiation to a desired cell type, typically making use of cues normally present during embryonic development (reviewed in Muguruma and Sasai, 2012). Indeed, when Shh was excluded from our culture conditions, eGFP+ neurons were completely absent upon differentiation of the *Dlx5/6*-eGFP line (Figure S3). There are, however, inherent limitations with using extrinsic factors to guide ES cell fate. Shh, for example, is a morphogen whose graded expression influences cell fate in a concentration and temporally regulated manner, making reiteration of the precise timing and levels of Shh exposure within an in vitro environment extremely difficult, if not impossible. Indeed, whereas differentiation of some neuronal cell classes (motor neurons and midbrain dopaminergic neurons most prominently) using extrinsic factors have met with success, other neuronal populations, including cINs have proven more problematic (Maroof et al., 2010). We therefore explored the possibility that intrinsic transcriptional specification might augment our baseline conditions for *Dlx5/6*-eGFP+ neuronal differentiation by normalizing cellular response to extrinsic cues. To do so, we generated two additional transgenic ES cell lines in which we could sequentially direct the expression of transcription factors relevant to cortical interneuron development in a manner recapitulating normal developmental expression.

Nkx2-1 is a homeodomain transcription factor whose expression in the medial ganglionic eminence is critical for neuronal identity. Its removal, even shortly before MGE cells become postmitotic, is sufficient to alter cell fate, switching interneurons from an MGE to a CGE fate (Butt et al., 2008). Conversely, sustained expression of *Nkx2-1* alters migratory behavior so that interneurons are retained ventrally and innervate instead the striatum (Nóbrega-Pereira et al., 2008). Thus, to recapitulate cIN development, it is important to tightly regulate *Nkx2-1* such that its expression is extinguished concomitant to the stage in vivo when cIN progenitors exit the subventricular zone. In order to mimic endogenous *Nkx2-1* regulation during cIN development, we employed the intron II regulatory element of *Nestin* (neural-specific *Nestin* enhancer) and a minimal promoter to regulate its expression (Figure S4) (Zimmerman et al., 1994). *Nestin* intron II is a widely used transgenic regulatory element, which is expressed in neural progenitors and is downregulated postmitotically. A similar approach was employed to drive the expression of *Lmx1a* in ES cells to direct their differentiation toward a midbrain dopaminergic cell fate (Andersson et al., 2006).

Another gene known to be important in cIN development is *Dlx2*, also a homeodomain transcription factor, which is tightly

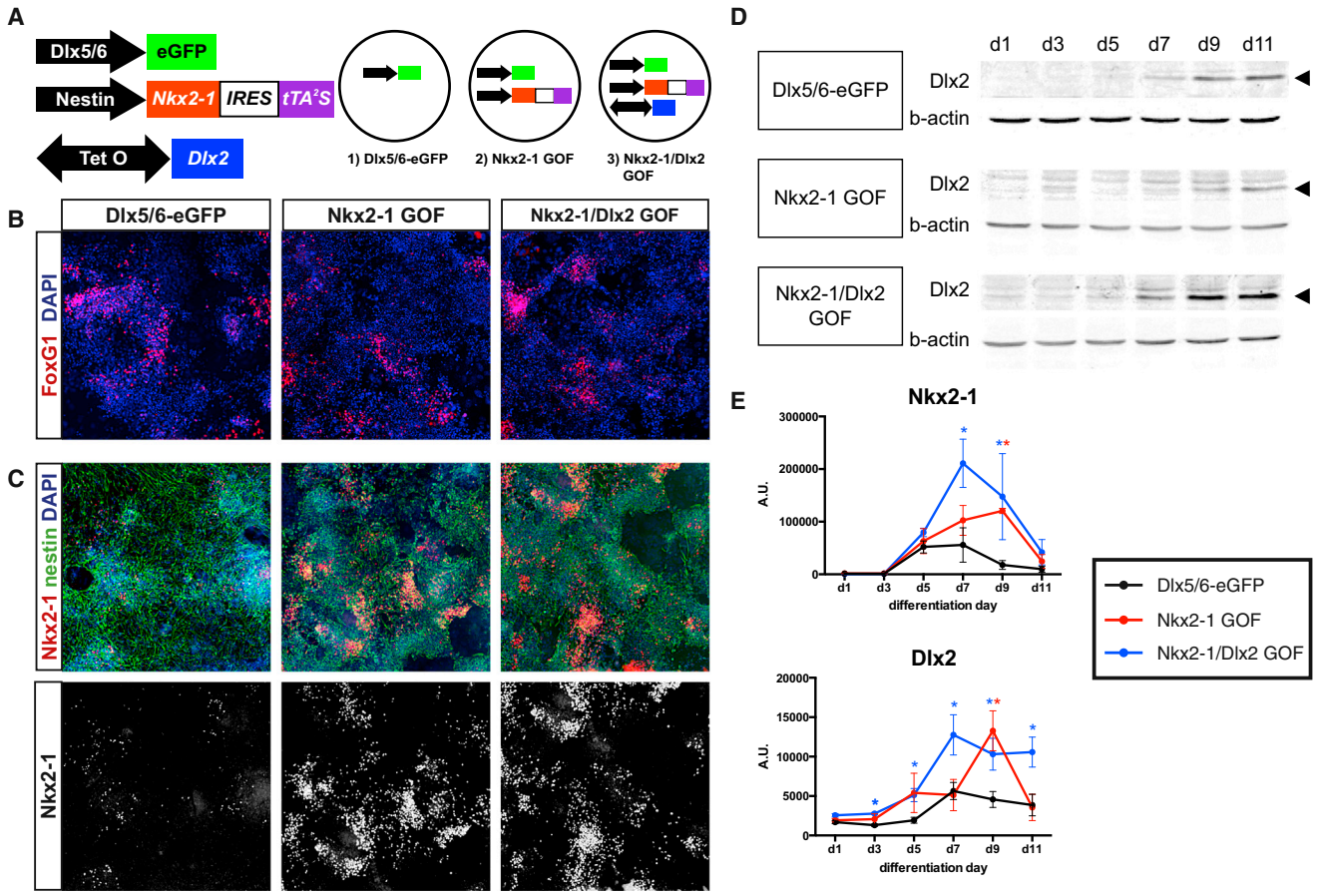

Figure 2. Directed Transcriptional Specification of Cortical Interneurons with Nkx2-1 and Dlx2

(A) Schematic representation of transgenes introduced into a wild-type ES cell line. A parental line was produced by introducing (1) eGFP under the control of the Dlx5/6 intergenic region and a minimal promoter. To the parental line, two additional transgenes were sequentially introduced: (2) *Nestin* intron II with minimal promoter driving Nkx2-1-IRES-tTA2S and (3) tetracycline response element driving Dlx2. Therefore, three separate stable ES lines were established containing 1, 2, or all 3 transgenes: (1) Dlx5/6-eGFP, (2) Nkx2-1 GOF, and (3) Nkx2-1/Dlx2 GOF, respectively.

(B) All three lines were differentiated for 11 days as embryoid bodies, and there was no observable difference in differentiation efficiency to telencephalic fate as measured by FoxG1.

(C) Nkx2-1 was strongly and broadly expressed in the large majority of nestin-expressing cells of Nkx2-1 GOF and Nkx2-1/Dlx2 GOF, whereas in Dlx5/6-eGFP, its expression was limited to small clusters.

(D) Time course of Dlx2 expression in differentiating embryoid bodies by western blot. Dlx5/6-eGFP and Nkx2-1GOF both begin expressing Dlx2 at day 7 and have similar expression levels. Nkx2-1/Dlx2 GOF expresses Dlx2 in a similar time course at elevated levels. β-actin loading controls below each Dlx2 blot.

(E) Quantification of Nkx2-1 and Dlx2 levels in embryoid bodies normalized to β-actin loading controls during in vitro differentiation. Red asterisk denotes $p < 0.05$ for Nkx2-1 GOF over Dlx5/6-eGFP. Blue asterisk denotes $p < 0.05$ for Nkx2-1/Dlx2 GOF over Dlx5/6-eGFP. Data represented as mean ± SEM.

See also Figures S2 and S4.

linked with GABAergic character and cIN migration (Anderson et al., 1997; Cobos et al., 2007; Stühmer et al., 2002a). Its expression within cortical interneuron lineages lags slightly behind *Nkx2-1*, initiated as progenitors enter the subventricular zone and is retained briefly after *Nkx2-1* has been extinguished (Eisenstat et al., 1999). To mimic this genetic cascade, we included a tetracycline transactivator element ($tTA2^s$) to be coexpressed along with *Nkx2-1* (Urlinger et al., 2000). As *Nestin* intron II becomes active, $tTA2^s$ levels will build up until a sufficient amount is produced to bind to the tetracycline responsive element (TRE), which drives the expression of Dlx2 in *trans*. Because *Nkx2-1* expression is induced under the influence of the neuronal nestin enhancer, while also producing $tTA2^s$, it results in delayed *Dlx2* induction, approximating the timing of expression of these genes found in vivo (Figure S4B). Although $tTA2^s$ transcription expires with the extinction of the *Nestin* enhancer, our hope was that the initial induction of Dlx2 would be sufficient to initiate the normal differentiation cascade seen in cINs.

To test this transcriptional specification strategy, we generated two transgenic ES cell lines using the *Dlx5/6*-eGFP reporter line as a starting point. The first line contains Nestin-*Nkx2-1*-IRES-$tTA2^s$ (*Nkx2-1* GOF), whereas the second contains both Nestin-Nkx2-1-IRES-$tTA2^s$ and TRE-*Dlx2* (Nkx2-1/Dlx2 GOF) (Figure 2A). This approach allowed us to gauge the relative contribution of Nkx2-1 alone, or the combined effects of both *Nkx2-1* and *Dlx2* on cIN differentiation in our reporter line.

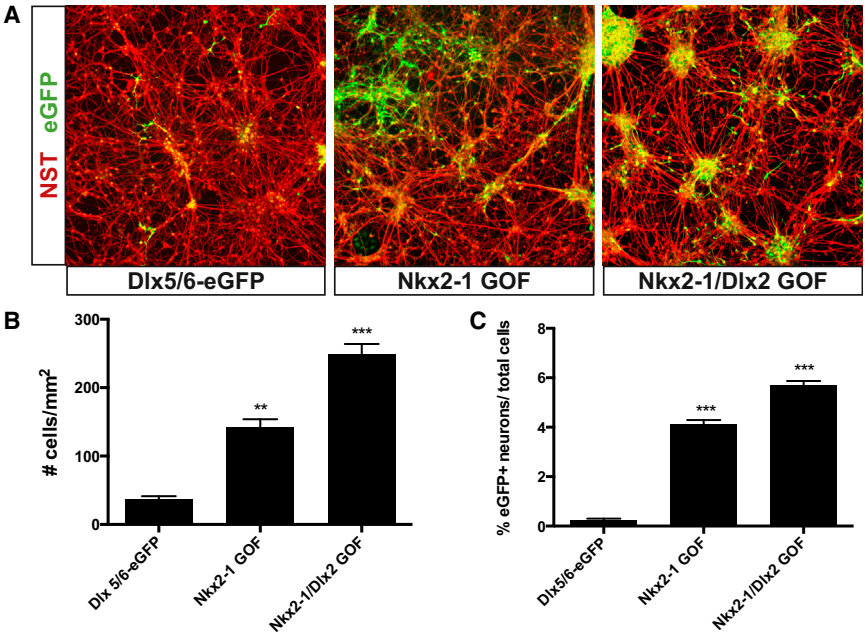

Figure 3. Transcriptional Specification with Nkx2-1 and Dlx2 Increases the Directed Production of Cortical Interneurons

(A) Representative images of neuronal monolayers generated from Dlx5/6-eGFP, Nkx2-1 GOF, and Nkx2-1/Dlx2 GOF lines; neuron-specific tubulin (red) and eGFP (green).

(B and C) Quantification of Dlx5/6-eGFP+ neurons by cell counts of 10× fields, normalized to mm^2 (B) or by FACS analysis (C), demonstrate a stepwise improvement in differentiation efficiency with Nkx2-1 GOF alone and Nkx2-1/Dlx2 GOF together. Dlx5/6-eGFP (IHC n = 6; FACS n = 4); Nkx2-1 GOF (IHC n = 5; FACS n = 4); Nkx2-1/Dlx2 GOF (IHC n = 5; FACS n = 4) (* $p < 0.05$; ** $p < 0.01$; *** $p < 0.001$). Data represented as mean ± SEM. See also Figures S2, S3, and S4.

To confirm that the transgenes were indeed resulting in increased expression of Nkx2-1 and Dlx2, embryoid bodies differentiated from all three lines were analyzed (Figures 2B–2D). We observed no noticeable difference in telencephalic progenitor specification across the three lines, as measured by FoxG1 expression (Figure 2B). This was expected as FoxG1 is upstream of both Nkx2-1 and Dlx2. However, in both Nkx2-1 GOF and Nkx2-1/Dlx2 GOF, there was a robust increase in Nkx2-1 expression (Figure 2E), largely coinciding with patches of nestin-positive neural progenitors (Figure 2C). To gauge Dlx2 expression, protein lysates were prepared from embryoid bodies at different time points during differentiation. Dlx2 expression was increased in the Nkx2-1/Dlx2 GOF line, and it also occurred slightly earlier (day 5) than in *Dlx5/6*-eGFP and Nkx2-1 GOF, where a Dlx2 band was detected starting at day 7 (Figure 2D). In the case of Nkx2-1, levels dropped back to baseline by day 11, but with Dlx2, elevated levels were sustained. These findings were confirmed by quantitative western analysis (Figure 2E), which shows a 3- to 4-fold increase in Nkx2-1 expression in Nkx2-1 GOF and Nkx2-1/Dlx2 GOF lines over Dlx5/6-eGFP reporter alone. This expression was dynamically regulated over the course of differentiation. Furthermore, Dlx2 induction was sustained in Nkx2-1/Dlx2 GOF beyond that of Nkx2-1 GOF.

In Vitro Differentiation of Transgenic ES Cell Lines

As before (Figure S2F), day 11 embryoid bodies were dissociated and plated onto laminin to generate neuronal monolayers. Prior to dissociation, there was already a noticeable difference in eGFP expression between *Dlx5/6*-eGFP embryoid bodies transcriptionally specified. Indeed, when embryoid bodies were freshly dissociated and quantified by fluorescence-activated cell sorting (FACs) analysis for eGFP, there was a significant increase in reporter gene induction between Dlx5/6-eGFP and Nkx2-1 GOF (Figure S3). Reporter gene expression in EBs was largely similar between Nkx2-1 GOF and Nkx2-1/Dlx2 GOF until progenitors were dissociated and differentiated into neuronal monolayers, at which point there was a clear difference between the three cell lines, as measured by immunohistochemistry and FACs analysis (Figure 3). Transcriptional specification by Nkx2-1 strongly increased the number of *Dlx5/6*-eGFP+ neurons by approximately 10-fold. *Dlx5/6*-eGFP expression was further augmented by Dlx2 gain of function, nearly doubling *Dlx5/6*-eGFP expression when compared with Nkx2-1 alone.

Transcriptional Specification Results in Increased cIN Output while Also Influencing Subtype Fate

We next examined the in vivo neuronal output of the three transgenic lines. As with the pan-eGFP line (Figure 1E), each line was differentiated, dissociated, and transplanted individually into host e13.5 MGE and analyzed postnatally. Because cINs must tangentially migrate a long distance away from the site of transplantation to reach the cortex, this transplantation paradigm serves as a rigorous biological "filter" for cells that have successfully differentiated into bona fide cortical interneurons.

The first difference we observed across the three transplant groups was in the numbers of cortical interneurons that successfully migrated dorsally into the cortex. Similar to the RCE transplant results (Figures 1F–1I), the reporter line alone (*Dlx5/6*-eGFP) resulted in a small number of sparsely distributed cINs. There was, however, a significant enhancement in the total number of cINs present in the cortex with Nkx2-1 GOF, an effect that mirrored the increase in Dlx5/6-eGFP+ neurons when the lines were differentiated in vivo. This effect was even greater with the addition of Dlx2 (Nkx2-1/Dlx2 GOF), for which we observed a further increase in the number of cINs that reached the cortex (Figure 4G). In all transplants, the cells present in the cortex exhibited complex morphologies similar to those observed in cINs in vivo at P21 (Figures 4E, 4F, and S5) and approximately 90% transplanted cells could be accounted for by cIN subtype markers (Figure S10B). Despite some variance

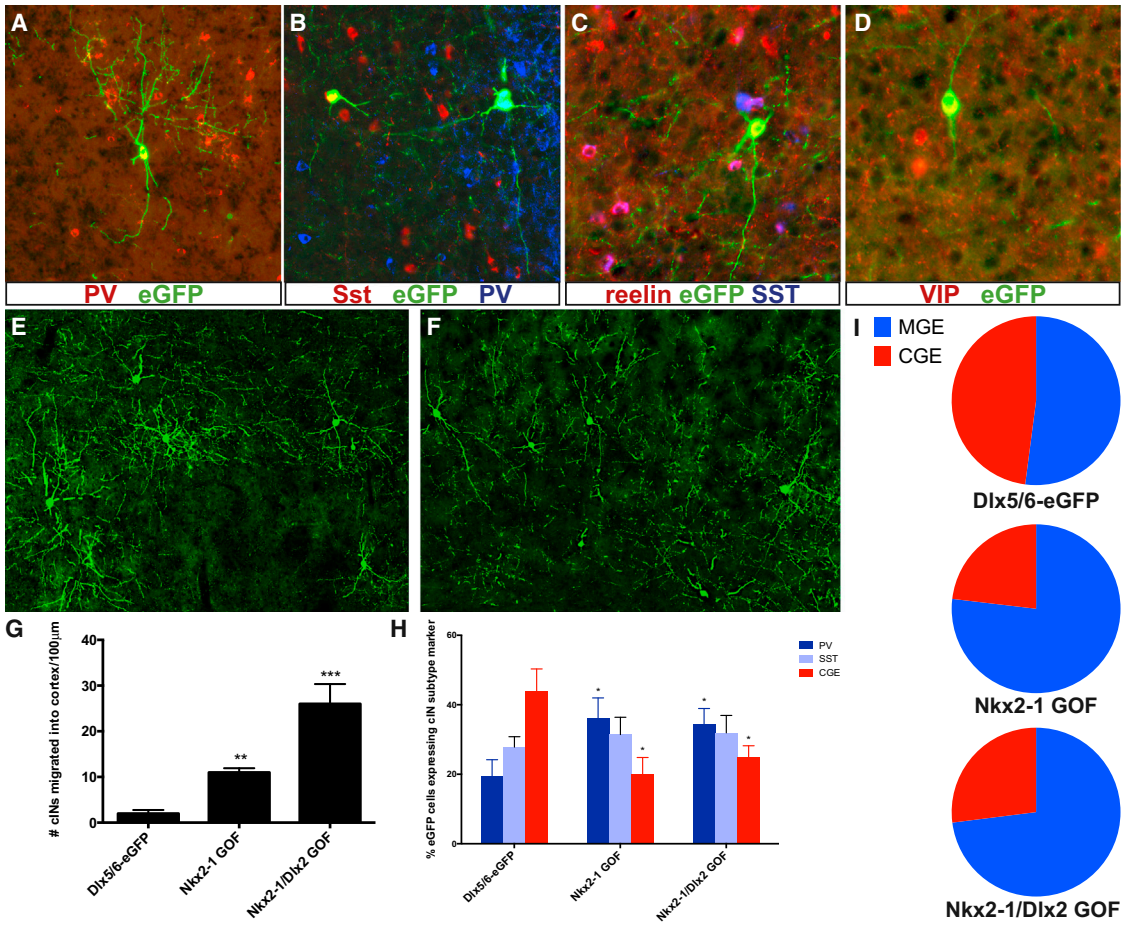

Figure 4. Transplantation of Three Differentiated Transgenic ES Lines Demonstrates the Effects of *Nkx2-1* and *Dlx2* on Cortical Interneuronal Differentiation

(A–D) Postnatal day 21 analysis of Dlx5/6-eGFP, Nkx2-1 GOF, and Nkx2-1/Dlx2 GOF were transplanted separately into e13.5 MGE and host animals. Examples of eGFP+ ES cell-derived cortical interneurons expressing parvalbumin (PV) (A and B), somatostatin (B and C), reelin-only (C), and vasointestinal peptide (D).

(E and F) Examples of groups of ES-derived cINs exhibiting complex morphologies consistent with bona fide cINs.

(G) Numbers of cINs present in the cortex quantified across the transgenic lines show a stepwise increase in migration efficiency with Nkx2-1 alone and Nkx-1/Dlx2 together.

(H and I) Quantification of cIN subtype markers expressed by transplanted cells demonstrates that Nkx2-1 strongly skews identity toward MGE-derived cINs, with no additional effects observed with the further addition of Dlx2. MGE versus CGE cIN subtypes summarized as pie charts in (I).

Dlx5/6-eGFP (n = 8; 388 cells); Nkx2-1 GOF (n = 7; 912 cells); Nkx2-1/Dlx2 GOF (n = 6, 1,281 cells) (* $p < 0.05$; ** $p < 0.01$; *** $p < 0.001$). Data represented as mean ± SEM.

See also Figures S5, S6, and S11.

in numbers between experiments, in all transplant groups the distribution of cINs was largely similar, both with respect to anterior-posterior and medial-lateral axes (Figure S5).

The second difference observed was in the cIN subtypes produced by the three transgenic cell lines. Cortical interneurons generated from the MGE and CGE are nonoverlapping populations, each readily distinguished by immunohistochemistry for parvalbumin, somatostatin, reelin, and vasointestinal peptide (VIP) (Figures 4A–4D). MGE-derived cINs express parvalbumin, somatostatin, or somatostatin/reelin. CGE-derived populations can be identified by their expression of either reelin (but lacking SST) or VIP (Miyoshi et al., 2010). In Dlx5/6-eGFP transplants we observed a near 1:1 ratio of both MGE and CGE class subtypes, as determined by immunohistochemistry, suggesting our baseline culture conditions did not bias toward either an MGE or CGE fate. There was, however, a significant enhancement (~75%) of MGE class cINs in both the Nkx2-1 GOF and Nkx2-1/Dlx2 GOF (Figures 4H and 4I). This was especially true of parvalbumin+ cINs, which significantly increased in proportion as a result of Nkx2-1 transcriptional specification (Figure 4H). Concomitantly, in both Nkx2-1 GOF and Nkx2-1/Dlx2 GOF conditions, CGE class reelin alone+ and VIP+ cINs were reduced as a proportion of the whole (Figure 4H). While under these conditions, there was a trend toward increased somatostatin+ MGE class cINs, but this did not reach statistical significance. Thus, in a gain-of-function context in ES cells, Nkx2-1 appears to

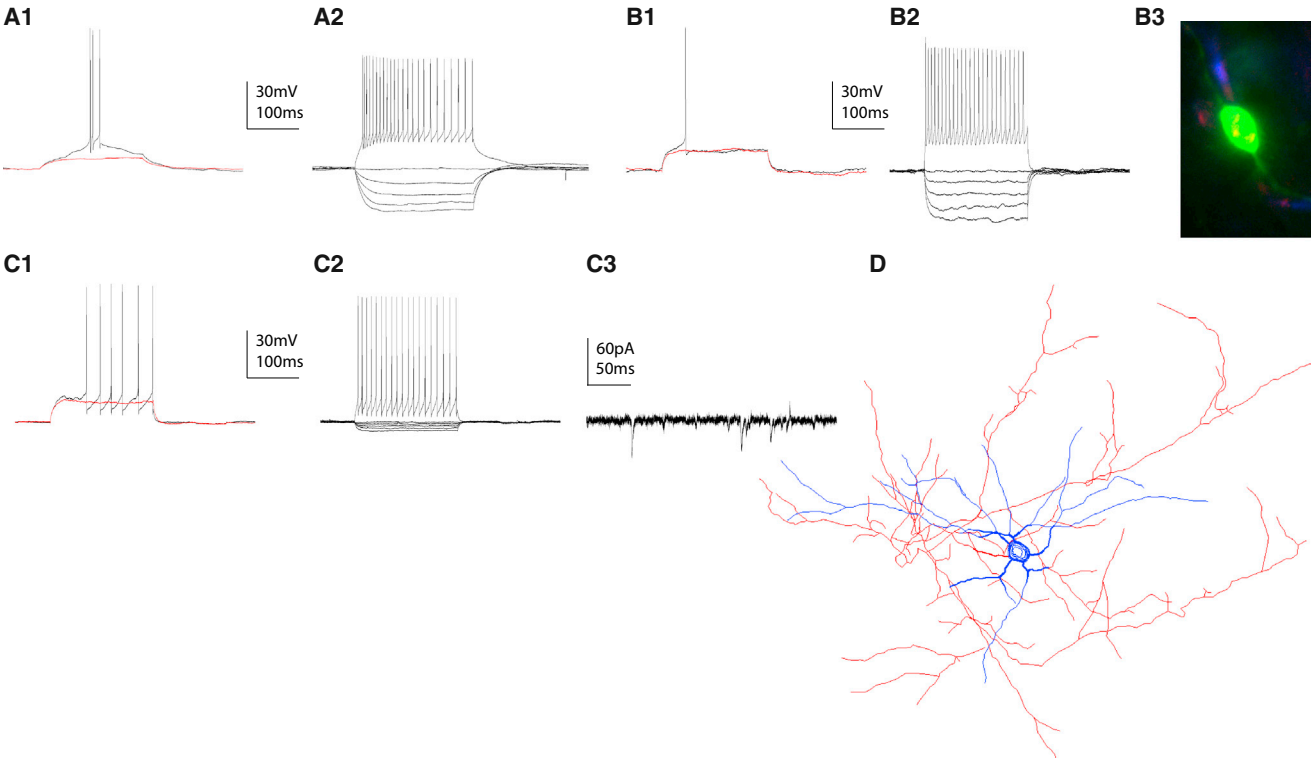

Figure 5. Proper Maturation of Transplanted ES Cells in the Neocortex

(A) Intrinsic electrophysiological properties of a transplanted ES-derived cIN, showing characteristics of a typical CGE-derived sigmoid intrinsic bursting cell (sIB). (A1) A burst of action potentials at threshold (black) and a pulse at just subthreshold depolarization (red). (A2) A series of hyperpolarizing voltage steps and a larger depolarizing one that leads to a higher frequency adapting discharge.

(B) Electrophysiological properties of a transcriptionally specified transplanted ES-derived cIN, showing characteristics of a typical MGE-derived non-fast-spiking cell (NFS). (B1) Threshold action potential discharge (black) and just subthreshold depolarization (red). B2) A series of hyperpolarizing voltage steps and a larger depolarizing one that leads to a higher frequency adapting discharge. (B3) The recorded cell was filled with biocytin (green) and was immunoreactive for somatostatin (red) and weakly for reelin (blue).

(C) Electrophysiological properties of a transcriptionally specified transplanted ES-derived cIN, showing characteristics of a typical MGE-derived delayed fast-spiking basket cell (dFS). (C1) Threshold action potential discharge (black) and just subthreshold depolarization (red). C2) A series of hyperpolarizing voltage steps and a larger depolarizing one that leads to a higher frequency nonadapting discharge. (C3) Incoming excitatory postsynaptic currents (EPSCs) recorded from the same cell at −65 mV.

(D) A morphological reconstruction of a transcriptionally specified and recorded ES-derived FS cell. The soma and dendrites are depicted in blue, whereas the axon in red. The axodendritic profile of the neuron displays characteristic features of FS cells, having an axon that bifurcates many times in the vicinity of the cell, bearing terminals that putatively contact surrounding other cell somata.

See also Figure S7.

positively regulate cIN fate, while also biasing the subtype specification toward MGE class interneurons. Additionally, transcriptional specification with both Nkx2.1 and Dlx2 did not have an additive effect on cIN subtype but did positively increase the numbers of cIN differentiation in general as measured by increased Dlx5/6-eGFP induction as well as increased tangential migration into the neocortex (Figure 4G).

Transplanted ES-Derived cINs Exhibit Normal Intrinsic Electrophysiological Properties

To bolster our analysis of transplanted cells, which had relied on marker expression and morphological characteristics, we tested for proper functional development and maturation of cIN identity by performing whole-cell patch-clamp electrophysiology on eGFP+ cells on acute brain slices cut from >P17 host mice. All the cells recorded in the three groups, Dlx5/6-eGFP, Nkx2-1 GOF, and Nkx2-1/Dlx2 GOF, displayed age-appropriate resting membrane potential (−63.73 ± 1.73) and exhibited intrinsic firing properties consistent with native cINs originating from MGE or CGE (Figure 5).

Specifically, when recording the Dlx5/6-eGFP-transplanted cells (n = 3), we identified two non-fast-spiking interneurons and one that possessed CGE-derived character, which we have previously described as a sigmoid bursting cell (sIB) (Miyoshi et al., 2010). This cell fired a burst of action potentials at low voltage threshold and upon further depolarization discharged in an adapting manner (Figure 5A).

When performing whole-cell recordings on transcriptionally specified cells (n = 23), consistent with their immunoprofile, the cells displayed action potential discharge patterns characteristic of both MGE- and CGE-derived cINs. In terms of the former, both typical fast-spiking basket cells (FS) and SOM-positive

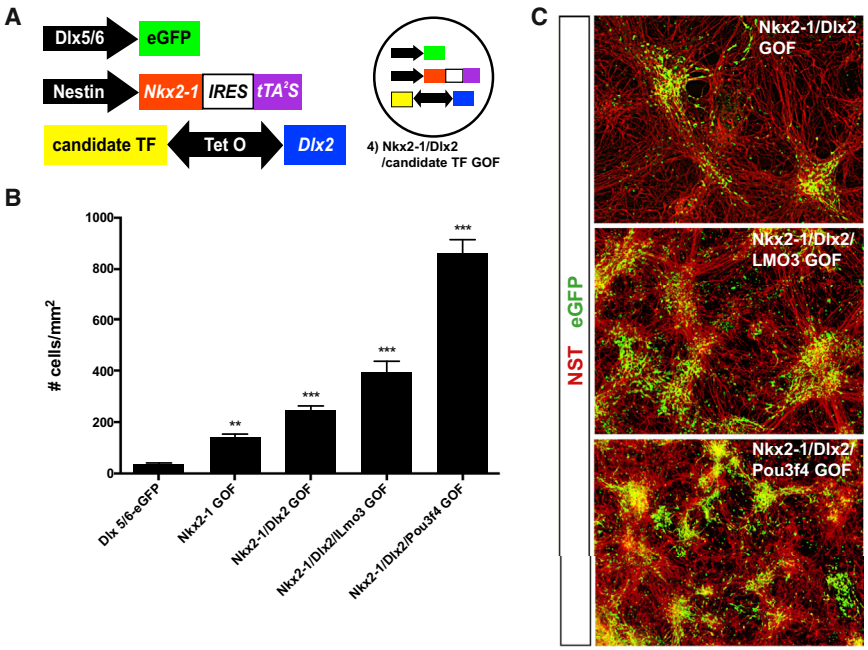

Figure 6. Using a Transcriptional Strategy to Test the Influence of Candidate Transcription Factors Revealed that LMO3 and Pou3f4 Affect the Subtype Identity and Induction of Cortical Interneurons

(A–C) Of the 12 candidate transcription factors tested, LMO3 and Pou3f4 most robustly improved Dlx5/6-eGFP+ neuronal differentiation above that achieved compared to the Nkx2-1/Dlx2 GOF baseline. (A) Candidate factors were introduced by utilizing the bidirectional nature of the tetracycline response element, allowing both Dlx2 and an additional factor to be simultaneously expressed under the control of tTA2S. (B) Dlx5/6-eGFP+ neurons were quantified by cell counts per 10× field, normalized to mm^2. (C) Representative field of Nkx2-1/Dlx2 GOF, Nkx2-1/Dlx2/LMO3 GOF, and Nkx2-1/Dlx2/Pou3f4 GOF; neuron-specific tubulin (NST; red) and eGFP (green). Nkx2-1/Dlx2/LMO3 GOF (IHC n = 4); Nkx2-1/Dlx2/Pou3f4 GOF (IHC n = 5) (* $p < 0.05$; ** $p < 0.01$; *** $p < 0.001$). Data represented as mean ± SEM.
See also Figures S8, S9, and S10.

non-fast-spiking cells (NFS) were identified (Figures 5B and 5C). The FS cells had an elaborate morphology (Figure 5D) and displayed a very short action potential half-width, sharp, and deep after hyperpolarization (AHP), and upon larger depolarization they were able to discharge at very high frequencies (Figure 5C; Table S1). In terms of the CGE-derived cINs, both bursting nonadapting (bNA) and late spiking cells were found, which have been shown to be VIP- and reelin-positive, respectively (Figure S7; Table S1). These results indicate that the transplanted cells undergo the normal time course for the development of passive and active intrinsic membrane properties. In addition, all the cells tested were found to receive spontaneous excitatory postsynaptic currents (sEPSCs) that had similar characteristics to those previously reported in the literature, demonstrating that the cells are embedded in the native network of neuronal connections (Figure 5C3).

Modular Gain of Function of Candidate Genes Identifies Three Factors that Enhance Either the Specificity or Efficiency of Cortical Interneurons Produced

Having established that *Nkx2-1* and *Dlx2* worked to improve cIN differentiation and skew toward an MGE subtype fate, we sought to use this system to identify novel transcription factors that influence the generation of specific subtypes of MGE-derived cINs. Our strategy for sequential expression of first Nkx2-1 and then Dlx2 is made possible by a tetracycline transactivator element binding to a bidirectional TRE (Figure S4B). Thus, by introducing a third transcription factor to the TRE that expresses in the opposite direction, another gene may be added to the cascade, coexpressed along with Dlx2 (Figures 6A and S8). To streamline this process, a Gateway destination cassette was introduced to the other end of the TRE, allowing for directional recombination of PCR products cloned into a Gateway entry vector. In this manner, 12 MGE-enriched transcription factors with unknown function (Figure S9) were cloned into the TRE-Dlx2 cassette and introduced into the Nestin-Nkx2-1-IRES-tTA ES cell line separately, resulting in the generation of 12 separate transgenic lines (Figure S8A). Importantly, none of the candidate genes tested had a noticeable effect on neuronal differentiation into monolayer cultures as assessed by NST labeling and density. Differentiation was gauged by Dlx5/6-eGFP expression, and the results are summarized in Table 1.

Of the genes tested, three significantly increased Dlx5/6-eGFP expression over baseline Nkx2-1/Dlx2 GOF (249 ± 33 cells/mm^2): *Pou3f4* GOF (834 ± 24 cells/mm^2), *Lmo3* GOF (397 ± 15 cells/mm^2), and *Zbtb20* GOF (428 ± 10 cells/mm^2) (Table 1). *Pou3f4* (also known as *Brn4*) exhibited a particularly strong effect on differentiation in vitro, resulting in approximately 35% Dlx5/6-eGFP+ neurons in the monolayer cultures, a 3.4-fold increase versus Nkx2-1/Dlx2 GOF (Figures 6B and 6C) and a 25-fold improvement compared to the absence of transcriptional specification (Figure S10).

An increase in Dlx5/6-eGFP expression may suggest that the candidate factor plays a role in cIN differentiation. To determine if this is in fact the case, we transplanted the *Nkx2-1/Dlx2/Lmo3* GOF line and analyzed transplanted cells postnatally at P21. Little is known about the function of *Lmo3* in the nervous system. The initial characterization of the *Lmo3* null mouse reported no obvious defects, and mutant animals were capable of normal breeding (Tse et al., 2004). In keeping with the in vitro differentiation results, Dlx5/6-eGFP proved to be a reliable predictor of tangential migration into the neocortex as the *Nkx2-1/Dlx2/Lmo3* GOF line had approximately 50% more cells in the cortex than did *Nkx2-1/Dlx2* gain-of-function alone (Figure 7B). We found at P21 that *Nkx2-1/Dlx2/Lmo3* GOF transplants contained a similar composition of MGE- and CGE-type cINs compared with *Nkx2-1/Dlx2* GOF (Figure S11). Within the MGE-type cINs,

Table 1. Quantitation of Dlx5/6-eGFP+ Neurons in Neuronal Monolayers as Influenced by Candidate Gene Transcriptional Specification

Candidate Gene	Number of Dlx5/6-eGFP+ Cells/mm^2 ± SD	Number of Clones Quantified	Number of Replicates
Nkx2-1/Dlx2 alone (no candidate gene)	249 ± 33	n/a	5
LMO1	225 ± 23	4	4
LMO3	397 ± 15	6	4
LMO4	263 ± 17	6	3
St18	195 ± 38	5	3
Glcci1	232 ± 33	7	3
Zbtb20	428 ± 10	6	4
Pou3f4	834 ± 24	5	5
Pou2f2	282 ± 30	4	3
Tox3	209 ± 12	4	3
Sox15	207 ± 10	6	3
Nfil3	188 ± 19	8	3
Mxd3	228 ± 38	7	3

however, we observed a significant shift: more of the cells were Pv+, and there was a trend toward fewer SST+ cINs (Figures 7B and S11). Overall, we observed an overrepresentation of Pv+ cells (a 3:1 ratio PV:SST). This suggested that of the two main MGE cIN subtypes, *Lmo3* might play a role in promoting Pv+ over SST+ identity.

We therefore analyzed the *Lmo3* null mouse (n = 5) as well as wild-type littermates (n = 4) to determine if parvalbumin+ and somatostatin+ cINs in the somatosensory cortex were affected. Wild-type littermate controls had numbers and distributions of parvalbumin and somatostatin in SS1 consistent with previous studies. By contrast, in *Lmo3* null animals the total number of Pv+ cINs was significantly reduced, and there was a slight increase in SST+ cINs (Figures 7C and 7D). Neither the overall number of MGE-type cINs nor their layer distribution was significantly altered in mutants (Figures 7D and S12A–S12C). Furthermore, neither proliferation at e13.5 as measured by BrDU nor Lhx6 in situ ventrally and in the cortex at e15.5 was noticeably different between *Lmo3* wild-type and null (Figures S13 and S14).

The overall effect was that in *Lmo3* null mice, Pv+ cells, which are normally the majority cIN type, were found in equal numbers to SST+ cells (a 1:1 ratio Pv:SST). The reduction in Pv+ cells was observed in all layers, while there was a trend toward increased SST+ cell numbers in layer V (Figures S12A–S12C). The 1:1 ratio of PV:SST was also observed in all layers (Figures S12D and S12E). Thus, the in vitro gain-of-function model of cIN development enabled us to reveal a previously unappreciated phenotype in the *Lmo3* null.

DISCUSSION

This study aimed to achieve three goals: (1) improving overall cortical interneuron differentiation by transcriptional specification, (2) taking the initial steps toward the generation of specific cIN subtypes by demonstrating that known factors influence cIN fate in an appropriate manner, and (3) creating an in vitro assay system whereby candidate transcription factors expressed embryonically can be systematically assayed for their effect on subtype specific differentiation. In each of these efforts, we have succeeded in significantly improving the efficient generation of specific cortical interneuron subtypes. Central to our approach was the desire to assess the cells we generated in the most physiologically rigorous manner possible. We thus challenged the cells generated through in utero transplantation and subsequent analysis of their ability to tangentially migrate into the neocortex, assume their normal morphological and marker expression profile, and perhaps most stringently, acquire their appropriate intrinsic electrophysiological properties. The strong correlation between our in vitro and in vivo assessments of cIN differentiation suggests that our methods provide a robust approach for the systematic identification of factors that are able to both augment and direct the differentiation of ES cells into specific cIN subtypes.

In making progress toward the first of these goals, we have demonstrated that ES cells can be differentiated into cortical interneurons using an established protocol for telencephalic differentiation. We also provided a demonstration that ES-derived cINs are capable of undergoing normal in vivo development, as assayed by in utero transplantation. Strikingly, ES-derived cINs were capable of undergoing long-range tangential migration into the cortex as well as morphological differentiation indistinguishable from cINs in vivo. They also exhibited proper intrinsic firing properties and mature cIN subtype marker expression. Transcriptional specification greatly improved differentiation efficiency when two well-established interneuron genes (known to be critical for cIN development) were introduced; *Nkx2-1* and *Dlx2*. Tangential migration as well as cIN subtype fate were also strongly influenced in a manner consistent with the established functions of these two transcription factors.

The central underlying logic to our approach is that developmental genetic analyses provide a framework for engineering the directed differentiation of cINs. Central to the intrinsic specification of cINs are *Nkx2-1* and the *Dlx* genes. *Nkx2-1* expression is very restricted in the embryonic brain, confined to the MGE, the ventral septum, and a small portion of the diencephalon. We and other groups have previously demonstrated the importance of *Nkx2-1* in cortical interneuron development, as well as its role in imparting MGE-like character to neurons generated from this structure (Butt et al., 2008; Sussel et al., 1999). Given its importance for cIN generation, it was somewhat surprising that *Nkx2-1* under the transcriptional control of a general neural enhancer element (*Nestin* intron II) did not provide a greater enhancement of *Dlx5/6*-eGFP expression, although our results are consistent with a recent study in which Nkx2-1 was inducibly regulated by doxycycline (Petros et al., 2013). One explanation is that *Nkx2-1* functions in a context dependent manner such that if the cells are not competent to respond to Nkx2-1, its mere presence is insufficient for it to function in specifying interneuron identity. Indeed, in nonneural structures, *Nkx2.1* is essential for both lung and thyroid development (Kimura et al., 1996; Minoo et al., 1999). In addition, the influence

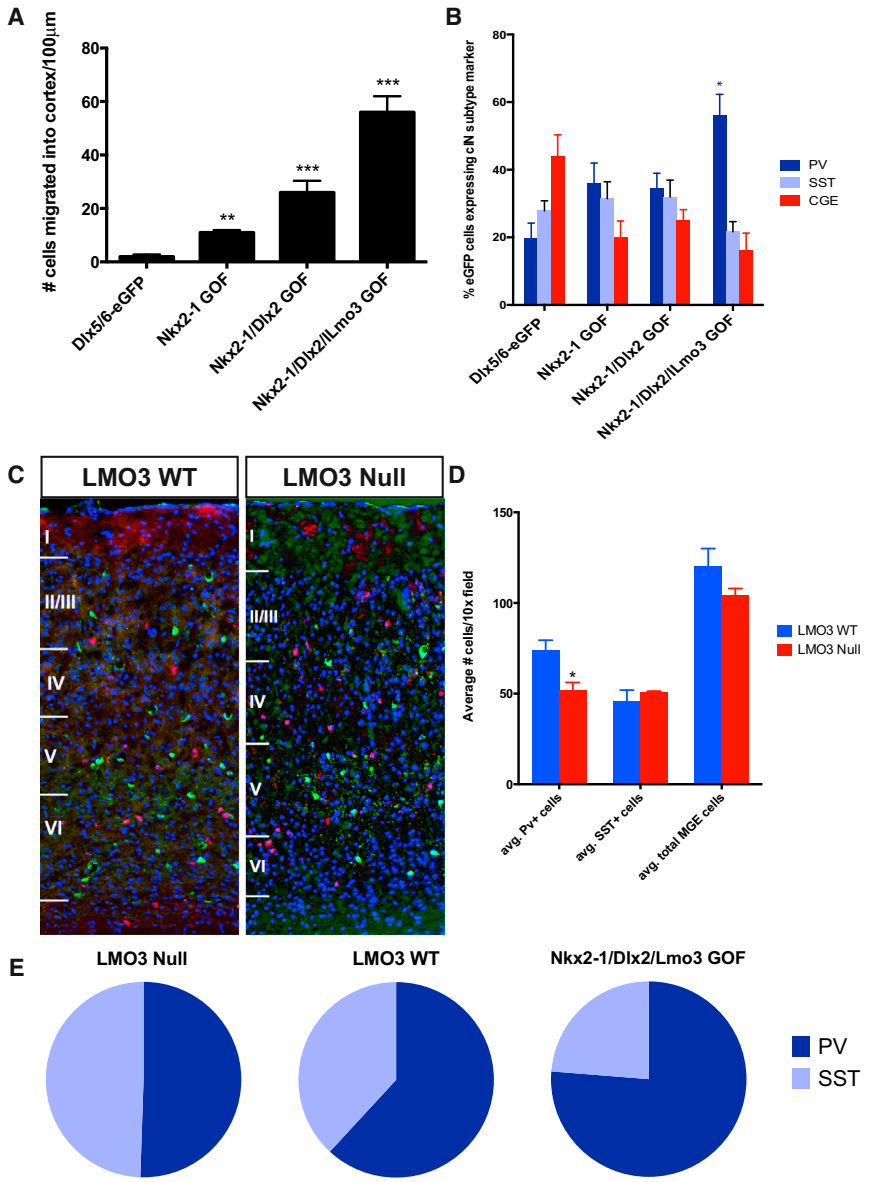

Figure 7. Analysis of the LMO3 Null Mouse Confirms the Prediction that LMO3 Plays a Role in Generating PV+ Cortical Interneurons

(A and B) Nkx2-1/Dlx2/LMO3 GOF line was differentiated and transplanted in utero into e13.5 MGE. Transplants were analyzed at P21 for numbers of cINs present in the cortex (A) as well as at cortical interneuron subtype marker expression. Nkx2-1/Dlx2/LMO3 GOF transplants displayed significant skew toward PV-expressing cINs (B).

(C and D) Analysis of LMO3 wild-type and LMO3 null mice showed that null animals have a significant decrease in Pv+ cINs, consistent with the transplant results (B).

(E) Summary of gain, loss, and normal expression of LMO3 on MGE cIN subtype fate. LMO3 WT (n=4); LMO3 null (n = 5) (* $p < 0.05$; ** $p < 0.01$; *** $p < 0.001$). Data represented as mean ± SEM.

See also Figures S11, S12, S13, and S14.

of *Nkx2-1* on cell fate is known to be temporally sensitive, so that if it is expressed too early or not sufficiently long enough, its influence on cellular identity and position varies. This idea is bolstered by findings in which genetic loss of function just prior or subsequent to exit from the cell cycle resulted in alternate cell fate or position (Butt et al., 2008; Nóbrega-Pereira et al., 2008). Indeed, we observed that not all cINs from the Nkx2-1 gain-of-function line adopted an MGE fate, as might have been predicted. This result emphasizes that even after the correct molecular determinants are identified, there remains a need for garnering maximal precision in the timing and level of their expression for optimizing directed cell fates. Nevertheless, transcriptional specification with Nkx2-1 was sufficient to drive some cIN differentiation in absence of Shh, whereas Dlx5/6-eGFP reporter line was dependent on exogenous Shh (Figure S3). The effect was only partial because the addition of Shh to the differentiation medium further enhanced differentiation efficiency and suggests perhaps that there exist other Shh-responsive factors independent of the Nkx2-1 transcriptional cascade.

Dlx2 expression is both broader and less temporally regulated than *Nkx2-1* and is expressed in interneurons later in their differentiation program (Eisenstat et al., 1999). *Dlx2* is expressed in most neurons generated from the subpallium, including the MGE, CGE, and LGE, and appears to be particularly important for the determination of GABAergic identity (Cobos et al., 2005; Stühmer et al., 2002a). By driving the expression of *Nkx2-1* before *Dlx2*, we hoped to recapitulate the normal order of gene expression and perhaps provide the cells with more specificity by first imparting them with MGE character. It is important to note that there is no direct evidence that the *Nkx2-1* transcriptional cascade is linked with *Dlx2* and that these two genes likely represent distinct but converging molecular cascades involved in cortical interneuron development. Consistent with this idea, we observed a near doubling of the number of *Dlx5/6*-eGFP+ neurons when both pathways were engaged. It also resulted in an approximate doubling in the number of ES-derived cINs found in the cortex at P21. The inclusion of *Dlx2* did not, however, impact cIN subtype fate, which is in agreement with the previously reported role of *Dlx2* in regulating cIN migration and specifying neuronal versus oligodendroglial fate (Petryniak et al., 2007). In this regard, it is notable that the *Dlx2* null mouse has a normal complement of MGE type cortical interneurons (Anderson et al., 1997; Qiu et al., 1995).

The observation that corecruitment of *Nkx2-1* and *Dlx2* greatly enhances the induction of cortical interneurons demonstrates that the directed differentiation of ES cells can be enhanced by

the appropriate use of genes known to play a role in cIN differentiation. By logical extension of these findings, we were able to optimize the genetic reprogramming strategy further by coexpressing candidate factors possibly involved in cortical interneuron development. This allowed us to test 12 genes unknown for their potential role in cIN in vitro differentiation. Three of these candidate genes significantly augmented *Dlx5/6*-eGFP expression over and above Nkx2-1/Dlx2 gain of function: *Lmo3*, *Pou3f4*, and *Zbtb20*. In particular, *Lmo3* gain-of-function, in addition to an approximate 60% increase in Dlx5/6-eGFP expression, also augmented the production of PV+ cINs accompanied by a decrease of the SST+ population. Our subsequent analysis of the *Lmo3* null animal revealed a significant reduction in Pv+ cINs and an increase in SST+ cINs without significantly affecting the overall number of MGE type cINs. Therefore, our in vitro gain-of-function model system accurately predicted a previously unreported phenotype in the *Lmo3* null mouse.

Although its role in interneuron specification had not been described, *Lmo3* has previously been described a target of *Arx* repression (Colasante et al., 2009; Friocourt and Parnavelas, 2011; Fulp et al., 2008). *Arx* itself has been implicated in a number of neurological disorders, including early onset epilepsy, and plays an important role in cIN migration (Friocourt and Parnavelas, 2010; Kitamura et al., 2002). However, despite the upregulation of *Lmo3* observed in *Arx* mutants, *Lmo3* gain of function did not phenocopy the migration deficits found in *Arx* null animals (Colasante et al., 2009). This is consistent with our findings that Lhx6 in situ was normal in e15.5 cortex (Figure S14), and layer distribution postnatally for Pv+ and SST+ cINs was normal in *Lmo3* null mice (Figures S12B–S12E). It will be interesting to employ our in vitro system to follow up on our findings and help provide insight mechanistically as to how *Lmo3* is acting on Pv+ cIN development.

Like *Lmo3*, *Pou3f4* dramatically increased differentiation efficiency (a 4.5-fold increase—approximately 35% *Dlx5/6*-eGFP+). Loss-of-function analysis of *Pou3f4* mutants, has not been implicated in the generation of cINs; rather, it has been associated with deafness in both mouse and humans (Kandpal et al., 1996; Minowa et al., 1999). It is interesting to note, however, that Pou3f4 has been reported to augment differentiation toward neural stem cells and dopaminergic neurons and might therefore act generally to enhance in vitro neural differentiation in the presence of other instructive intrinsic cues (Han et al., 2012; Tan et al., 2011). This is consistent with the overall broad expression exhibited by Pou3f4 in the embryonic brain. Taken together, our work highlights that loss of function per se may not always provide the most robust approach for identifying genes that have utility in the induction of specific neuronal subtypes, including cortical interneurons. At the very least, our findings indicate that complementing loss-of-function analysis with gain-of-function approaches will be highly fruitful as a means to identify genes that facilitate the generation of particular cIN subtypes. Thus, we anticipate that this model system can be broadly employed to systematically assay genes developmentally expressed in the MGE, with the aim that large numbers of specific, pure populations of cortical interneuron subtypes can be generated in future.

There is increasing evidence to suggest that cortical interneurons play a significant role in the etiology of numerous neuropsychiatric disorders. Their role in normal brain function is an area of intense study and, given their large diversity as a neuronal population, it is perhaps unsurprising to find that they are involved in a multitude of different circuits, impacting and shaping information coding and processing. Hence, we believe the approach we present will be of great value not only for allowing the generation of cortical interneurons in large numbers in vitro but to do so in a manner that permits their identity to be directed to specific subtype identities. As little is known about how individual subclasses of cINs are specified, such approaches depend upon identification of critical transcriptional cascades that underlie their diversity. As such, our development of a high-throughput approach for examining the function of candidate factors provides a robust method for identifying such factors. The potential to follow up such molecules through genetic and biochemical analysis provides a promising starting point for drug discovery, as well as for studying the contribution of novel genes to both normal and abnormal brain function.

EXPERIMENTAL PROCEDURES

ES Cell Differentiation

Differentiation of ES cells to become cINs was adapted from a protocol previously described for generating telencephalic precursors (Watanabe et al., 2005). Briefly, ES cells were maintained for two passages on gelatin (Millipore) in the absence of feeder layer cells prior to differentiation. Cells were then passaged with 0.05% trypsin-EDTA (Invitrogen) and added to the center of the well (35,000 cells/well) of a non-TC-treated 24-well plate (BD Falcon) containing 800 μl of "SFEB medium" (Glasgow's Minimal Essential Medium with KnockOut Serum Replacement [both from Invitrogen]) and Dkk-1 (R&D Systems; 25 ng/ml), designated day 0. Care was taken not to disturb the cells in the center of the well as they aggregated into embryoid bodies (EBs). On day 4, EBs and medium were transferred to 1.2 ml microtiter tubes (USA Scientific) and allowed to settle to the bottom. Old SFEB medium was removed, and 800 μl of new SFEB containing Dkk-1 and SHH N terminus (R&D Systems; 5 mM) was added. EBs and new medium were then returned to the 24-well plate for further differentiation. On day 6, SFEB medium was changed again, and Dkk-1 was no longer added to SFEB. Medium was changed similarly every 3 days until day 11, at which point embryoid bodies were dissociated for subsequent experiments.

Processing Cells for Immunohistochemistry

For imaging differentiating embryoid bodies, day 3 EBs were gently and incompletely dissociated with Accutase (StemGent) (10 min, 37°C followed by gentle trituration with P200 tip 5–10×) and plated on 4-chambered slides coated with poly-L-lysine/fibronectin at a 60,000 cells/cm^2. Adherent cells were grown in the same medium (SFEB) as floating embryoid body cultures. Medium was changed at the same intervals. At day 11, adherent cultures were fixed with 4% PFA for immunohistochemistry.

For neuronal monolayer cultures, day 11 EBs were gently and completely dissociated with Accutase (15 min, 37°C followed by gentle trituration with P200 tip 10–15×) and plated at 200,000 cells/cm^2 on poly-L-lysine/laminin and maintained in Neurobasal + B27 medium. Five days postplating, neurons were fixed for immunocytochemistry (see the Supplemental Experimental Procedures for more detail).

Cell Transplantation

A detailed description of ultrasound backscatter-guided transplantation has been described previously (Liu et al., 1998; Nery et al., 2002; Wichterle et al., 1999, 2001). Briefly, day 9 EBs were gently dissociated with Accutase (15 min, 37°C followed by gentle trituration with a P200 tip) and then incubated

with adenoassociated virus encoding CAG-eGFP for 3 hr in suspension. Medium was then changed, and by this point the cells were already reaggregated into EBs. At day 11 SFEBs were incompletely dissociated with Accutase (10 min, 37°C followed by gentle trituration with P1000 tip 5–10×), spun down 270 × g for 5 min, resuspended into a dense slurry of 500,000 cells/μl in Neurobasal + B27 + 0.001 U/ml DNase, and stored on ice.

Cells were frontloaded (Narishige MO-10 micromainpulator) into a pulled and sharpened glass pipette (carefully beveled with a microgrinder (Narishige) to 25°, creating an opening of approximately 30 μm), and delivered into the MGE of e13.5 Swiss Webster embryos using ultrasound-guided backscatter microscopy with the Vevo 770 system (VisualSonics, 40 MHz probe 704). Following surgery, the uterus was carefully replaced, and the dam was sewn up, allowing host pups to be birthed normally. At postnatal day 21, host animals were anesthetized and transcardially perfused in preparation for immunohistochemical analysis. Alternately, they were euthanized at postnatal day 18 and processed for slice electrophysiology. Number of replicates per transplant group used for cIN subtype analysis by immunohistochemistry (IHC): RCE n = 6; Dlx5/6-eGFP n = 8, 388 cells; Nkx2-1 GOF n = 7, 912 cells; Nkx2-1/Dlx2 GOF n = 6, 1,281 cells; Nkx2-1/Dlx2/LMO3 GOF n = 7, 1196 cells.

To control for unwanted AAV infection of host tissue, cells were labeled and dissociated for transplant as described above and then spun down at 13,000 × g for 10 min, killing the cells (assessed by typan blue staining). The resultant pellet was similarly resuspended and transplanted. No eGFP+ cells were observed in such transplants in the transplant site or in the cortex at P21. For neural stem cell transplants (Sox1-eGFP ES cell line), embryoid bodies were partially dissociated at day 4, labeled with GFP-AAV, and allowed to reaggregate. At day 6 cells were similarly transplanted into e13.5 MGE in utero as described above. In parallel, *Sox1*-eGFP EBs were partially dissociated at day 4 and reaggregated without AAV. These cells were then analyzed by FACs at day 6 to gauge differentiation efficiency (>90% *Sox1*-eGFP+).

SUPPLEMENTAL INFORMATION

Supplemental Information includes Supplemental Experimental Procedures, 14 figures, and one table and can be found with this article online at http://dx.doi.org/10.1016/j.neuron.2013.09.022.

ACKNOWLEDGMENTS

We thank Austin Smith (University of Cambridge) for the Sox1-eGFP ES line, Yoshiki Sasai (RIKEN, Kobe) for the Bf-1 antibody, Marc Fucillo for training with UBM transplants, and Fishell lab members (Melissa McKenzie-Chang and Tim Petros, in particular) for their feedback and critical reading of our manuscript. This work was supported by NYSTEM (C024326), grants from the National Institute of Health (MH071679, MH095147, NS074972, NS081297 (G.F.), generous support from the Simons Foundation (G.F.), and a CIHR fellowship (to E.A.).

Accepted: September 11, 2013
Published: December 4, 2013

REFERENCES

Anderson, S.A., Eisenstat, D.D., Shi, L., and Rubenstein, J.L. (1997). Interneuron migration from basal forebrain to neocortex: dependence on Dlx genes. Science *278*, 474–476.

Andersson, E., Tryggvason, U., Deng, Q., Friling, S., Alekseenko, Z., Robert, B., Perlmann, T., and Ericson, J. (2006). Identification of intrinsic determinants of midbrain dopamine neurons. Cell *124*, 393–405.

Andrews, G.L., Yun, K., Rubenstein, J.L., and Mastick, G.S. (2003). Dlx transcription factors regulate differentiation of dopaminergic neurons of the ventral thalamus. Mol. Cell. Neurosci. *23*, 107–120.

Ascoli, G.A., Alonso-Nanclares, L., Anderson, S.A., Barrionuevo, G., Benavides-Piccione, R., Burkhalter, A., Buzsáki, G., Cauli, B., Defelipe, J., Fairén, A., et al.; Petilla Interneuron Nomenclature Group (2008). Petilla terminology: nomenclature of features of GABAergic interneurons of the cerebral cortex. Nat. Rev. Neurosci. *9*, 557–568.

Belforte, J.E., Zsiros, V., Sklar, E.R., Jiang, Z., Yu, G., Li, Y., Quinlan, E.M., and Nakazawa, K. (2010). Postnatal NMDA receptor ablation in corticolimbic interneurons confers schizophrenia-like phenotypes. Nat. Neurosci. *13*, 76–83.

Butt, S.J., Fuccillo, M., Nery, S., Noctor, S., Kriegstein, A., Corbin, J.G., and Fishell, G. (2005). The temporal and spatial origins of cortical interneurons predict their physiological subtype. Neuron *48*, 591–604.

Butt, S.J., Sousa, V.H., Fuccillo, M.V., Hjerling-Leffler, J., Miyoshi, G., Kimura, S., and Fishell, G. (2008). The requirement of Nkx2-1 in the temporal specification of cortical interneuron subtypes. Neuron *59*, 722–732.

Cardin, J.A., Carlén, M., Meletis, K., Knoblich, U., Zhang, F., Deisseroth, K., Tsai, L.H., and Moore, C.I. (2009). Driving fast-spiking cells induces gamma rhythm and controls sensory responses. Nature *459*, 663–667.

Chao, H.T., Chen, H., Samaco, R.C., Xue, M., Chahrour, M., Yoo, J., Neul, J.L., Gong, S., Lu, H.C., Heintz, N., et al. (2010). Dysfunction in GABA signalling mediates autism-like stereotypies and Rett syndrome phenotypes. Nature *468*, 263–269.

Cobos, I., Calcagnotto, M.E., Vilaythong, A.J., Thwin, M.T., Noebels, J.L., Baraban, S.C., and Rubenstein, J.L. (2005). Mice lacking Dlx1 show subtype-specific loss of interneurons, reduced inhibition and epilepsy. Nat. Neurosci. *8*, 1059–1068.

Cobos, I., Borello, U., and Rubenstein, J.L. (2007). Dlx transcription factors promote migration through repression of axon and dendrite growth. Neuron *54*, 873–888.

Colasante, G., Sessa, A., Crispi, S., Calogero, R., Mansouri, A., Collombat, P., and Broccoli, V. (2009). Arx acts as a regional key selector gene in the ventral telencephalon mainly through its transcriptional repression activity. Dev. Biol. *334*, 59–71.

Curley, A.A., and Lewis, D.A. (2012). Cortical basket cell dysfunction in schizophrenia. J. Physiol. *590*, 715–724.

Eiraku, M., Watanabe, K., Matsuo-Takasaki, M., Kawada, M., Yonemura, S., Matsumura, M., Wataya, T., Nishiyama, A., Muguruma, K., and Sasai, Y. (2008). Self-organized formation of polarized cortical tissues from ESCs and its active manipulation by extrinsic signals. Cell Stem Cell *3*, 519–532.

Eisenstat, D.D., Liu, J.K., Mione, M., Zhong, W., Yu, G., Anderson, S.A., Ghattas, I., Puelles, L., and Rubenstein, J.L. (1999). DLX-1, DLX-2, and DLX-5 expression define distinct stages of basal forebrain differentiation. J. Comp. Neurol. *414*, 217–237.

Fazzari, P., Paternain, A.V., Valiente, M., Pla, R., Luján, R., Lloyd, K., Lerma, J., Marín, O., and Rico, B. (2010). Control of cortical GABA circuitry development by Nrg1 and ErbB4 signalling. Nature *464*, 1376–1380.

Fino, E., and Yuste, R. (2011). Dense inhibitory connectivity in neocortex. Neuron *69*, 1188–1203.

Friocourt, G., and Parnavelas, J.G. (2010). Mutations in ARX result in several defects involving GABAergic neurons. Front. Cell. Neurosci. *4*, 4.

Friocourt, G., and Parnavelas, J.G. (2011). Identification of Arx targets unveils new candidates for controlling cortical interneuron migration and differentiation. Front. Cell. Neurosci. *5*, 28.

Fulp, C.T., Cho, G., Marsh, E.D., Nasrallah, I.M., Labosky, P.A., and Golden, J.A. (2008). Identification of Arx transcriptional targets in the developing basal forebrain. Hum. Mol. Genet. *17*, 3740–3760.

Gaspard, N., Bouschet, T., Hourez, R., Dimidschstein, J., Naeije, G., van den Ameele, J., Espuny-Camacho, I., Herpoel, A., Passante, L., Schiffmann, S.N., et al. (2008). An intrinsic mechanism of corticogenesis from embryonic stem cells. Nature *455*, 351–357.

Han, D.W., Tapia, N., Hermann, A., Hemmer, K., Höing, S., Araúzo-Bravo, M.J., Zaehres, H., Wu, G., Frank, S., Moritz, S., et al. (2012). Direct reprogramming of fibroblasts into neural stem cells by defined factors. Cell Stem Cell *10*, 465–472.

Kandpal, G., Jacob, A.N., and Kandpal, R.P. (1996). Transcribed sequences encoded in the region involved in contiguous deletion syndrome that

comprises X-linked stapes fixation and deafness. Somat. Cell Mol. Genet. *22*, 511–517.

Kawaguchi, Y., and Kondo, S. (2002). Parvalbumin, somatostatin and cholecystokinin as chemical markers for specific GABAergic interneuron types in the rat frontal cortex. J. Neurocytol. *31*, 277–287.

Kimura, S., Hara, Y., Pineau, T., Fernandez-Salguero, P., Fox, C.H., Ward, J.M., and Gonzalez, F.J. (1996). The T/ebp null mouse: thyroid-specific enhancer-binding protein is essential for the organogenesis of the thyroid, lung, ventral forebrain, and pituitary. Genes Dev. *10*, 60–69.

Kitamura, K., Yanazawa, M., Sugiyama, N., Miura, H., Iizuka-Kogo, A., Kusaka, M., Omichi, K., Suzuki, R., Kato-Fukui, Y., Kamiirisa, K., et al. (2002). Mutation of ARX causes abnormal development of forebrain and testes in mice and X-linked lissencephaly with abnormal genitalia in humans. Nat. Genet. *32*, 359–369.

Klausberger, T., and Somogyi, P. (2008). Neuronal diversity and temporal dynamics: the unity of hippocampal circuit operations. Science *321*, 53–57.

Konradi, C., Yang, C.K., Zimmerman, E.I., Lohmann, K.M., Gresch, P., Pantazopoulos, H., Berretta, S., and Heckers, S. (2011). Hippocampal interneurons are abnormal in schizophrenia. Schizophr. Res. *131*, 165–173.

Kvitsiani, D., Ranade, S., Hangya, B., Taniguchi, H., Huang, J.Z., and Kepecs, A. (2013). Distinct behavioural and network correlates of two interneuron types in prefrontal cortex. Nature *498*, 363–366.

Lapray, D., Lasztoczi, B., Lagler, M., Viney, T.J., Katona, L., Valenti, O., Hartwich, K., Borhegyi, Z., Somogyi, P., and Klausberger, T. (2012). Behavior-dependent specialization of identified hippocampal interneurons. Nat. Neurosci. *15*, 1265–1271.

Lee, S., Cuvillier, J.M., Lee, B., Shen, R., Lee, J.W., and Lee, S.K. (2012). Fusion protein Isl1-Lhx3 specifies motor neuron fate by inducing motor neuron genes and concomitantly suppressing the interneuron programs. Proc. Natl. Acad. Sci. USA *109*, 3383–3388.

Liu, A., Joyner, A.L., and Turnbull, D.H. (1998). Alteration of limb and brain patterning in early mouse embryos by ultrasound-guided injection of Shh-expressing cells. Mech. Dev. *75*, 107–115.

Maroof, A.M., Brown, K., Shi, S.H., Studer, L., and Anderson, S.A. (2010). Prospective isolation of cortical interneuron precursors from mouse embryonic stem cells. J. Neurosci. *30*, 4667–4675.

Maroof, A.M., Keros, S., Tyson, J.A., Ying, S.W., Ganat, Y.M., Merkle, F.T., Liu, B., Goulburn, A., Stanley, E.G., Elefanty, A.G., et al. (2013). Directed differentiation and functional maturation of cortical interneurons from human embryonic stem cells. Cell Stem Cell *12*, 559–572.

Martinat, C., Bacci, J.J., Leete, T., Kim, J., Vanti, W.B., Newman, A.H., Cha, J.H., Gether, U., Wang, H., and Abeliovich, A. (2006). Cooperative transcription activation by Nurr1 and Pitx3 induces embryonic stem cell maturation to the midbrain dopamine neuron phenotype. Proc. Natl. Acad. Sci. USA *103*, 2874–2879.

Mazzoni, E.O., Mahony, S., Closser, M., Morrison, C.A., Nedelec, S., Williams, D.J., An, D., Gifford, D.K., and Wichterle, H. (2013). Synergistic binding of transcription factors to cell-specific enhancers programs motor neuron identity. Nat. Neurosci. *16*, 1219–1227.

Minoo, P., Su, G., Drum, H., Bringas, P., and Kimura, S. (1999). Defects in tracheoesophageal and lung morphogenesis in Nkx2.1(-/-) mouse embryos. Dev. Biol. *209*, 60–71.

Minowa, O., Ikeda, K., Sugitani, Y., Oshima, T., Nakai, S., Katori, Y., Suzuki, M., Furukawa, M., Kawase, T., Zheng, Y., et al. (1999). Altered cochlear fibrocytes in a mouse model of DFN3 nonsyndromic deafness. Science *285*, 1408–1411.

Miyoshi, G., Hjerling-Leffler, J., Karayannis, T., Sousa, V.H., Butt, S.J., Battiste, J., Johnson, J.E., Machold, R.P., and Fishell, G. (2010). Genetic fate mapping reveals that the caudal ganglionic eminence produces a large and diverse population of superficial cortical interneurons. J. Neurosci. *30*, 1582–1594.

Muguruma, K., and Sasai, Y. (2012). In vitro recapitulation of neural development using embryonic stem cells: from neurogenesis to histogenesis. Dev. Growth Differ. *54*, 349–357.

Nery, S., Fishell, G., and Corbin, J.G. (2002). The caudal ganglionic eminence is a source of distinct cortical and subcortical cell populations. Nat. Neurosci. *5*, 1279–1287.

Nicholas, C.R., Chen, J., Tang, Y., Southwell, D.G., Chalmers, N., Vogt, D., Arnold, C.M., Chen, Y.J., Stanley, E.G., Elefanty, A.G., et al. (2013). Functional maturation of hPSC-derived forebrain interneurons requires an extended timeline and mimics human neural development. Cell Stem Cell *12*, 573–586.

Nóbrega-Pereira, S., Kessaris, N., Du, T., Kimura, S., Anderson, S.A., and Marín, O. (2008). Postmitotic Nkx2-1 controls the migration of telencephalic interneurons by direct repression of guidance receptors. Neuron *59*, 733–745.

Panman, L., Andersson, E., Alekseenko, Z., Hedlund, E., Kee, N., Mong, J., Uhde, C.W., Deng, Q., Sandberg, R., Stanton, L.W., et al. (2011). Transcription factor-induced lineage selection of stem-cell-derived neural progenitor cells. Cell Stem Cell *8*, 663–675.

Petros, T.J., Maurer, C.W., and Anderson, S.A. (2013). Enhanced derivation of mouse ESC-derived cortical interneurons by expression of Nkx2.1. Stem Cell Res. (Amst.) *11*, 647–656.

Petryniak, M.A., Potter, G.B., Rowitch, D.H., and Rubenstein, J.L. (2007). Dlx1 and Dlx2 control neuronal versus oligodendroglial cell fate acquisition in the developing forebrain. Neuron *55*, 417–433.

Qiu, M., Bulfone, A., Martinez, S., Meneses, J.J., Shimamura, K., Pedersen, R.A., and Rubenstein, J.L. (1995). Null mutation of Dlx-2 results in abnormal morphogenesis of proximal first and second branchial arch derivatives and abnormal differentiation in the forebrain. Genes Dev. *9*, 2523–2538.

Son, E.Y., Ichida, J.K., Wainger, B.J., Toma, J.S., Rafuse, V.F., Woolf, C.J., and Eggan, K. (2011). Conversion of mouse and human fibroblasts into functional spinal motor neurons. Cell Stem Cell *9*, 205–218.

Sousa, V.H., Miyoshi, G., Hjerling-Leffler, J., Karayannis, T., and Fishell, G. (2009). Characterization of Nkx6-2-derived neocortical interneuron lineages. Cereb. Cortex *19* (*Suppl 1*), i1–i10.

Stenman, J., Toresson, H., and Campbell, K. (2003). Identification of two distinct progenitor populations in the lateral ganglionic eminence: implications for striatal and olfactory bulb neurogenesis. J. Neurosci. *23*, 167–174.

Stühmer, T., Anderson, S.A., Ekker, M., and Rubenstein, J.L. (2002a). Ectopic expression of the Dlx genes induces glutamic acid decarboxylase and Dlx expression. Development *129*, 245–252.

Stühmer, T., Puelles, L., Ekker, M., and Rubenstein, J.L. (2002b). Expression from a Dlx gene enhancer marks adult mouse cortical GABAergic neurons. Cereb. Cortex *12*, 75–85.

Sussel, L., Marin, O., Kimura, S., and Rubenstein, J.L. (1999). Loss of Nkx2.1 homeobox gene function results in a ventral to dorsal molecular respecification within the basal telencephalon: evidence for a transformation of the pallidum into the striatum. Development *126*, 3359–3370.

Tan, X.F., Jin, G.H., Tian, M.L., Qin, J.B., Zhang, L., Zhu, H.X., and Li, H.M. (2011). The co-transduction of Nurr1 and Brn4 genes induces the differentiation of neural stem cells into dopaminergic neurons. Cell Biol. Int. *35*, 1217–1223.

Tse, E., Smith, A.J., Hunt, S., Lavenir, I., Forster, A., Warren, A.J., Grutz, G., Foroni, L., Carlton, M.B., Colledge, W.H., et al. (2004). Null mutation of the Lmo4 gene or a combined null mutation of the Lmo1/Lmo3 genes causes perinatal lethality, and Lmo4 controls neural tube development in mice. Mol. Cell. Biol. *24*, 2063–2073.

Urlinger, S., Baron, U., Thellmann, M., Hasan, M.T., Bujard, H., and Hillen, W. (2000). Exploring the sequence space for tetracycline-dependent transcriptional activators: novel mutations yield expanded range and sensitivity. Proc. Natl. Acad. Sci. USA *97*, 7963–7968.

Wang, A.Y., Lohmann, K.M., Yang, C.K., Zimmerman, E.I., Pantazopoulos, H., Herring, N., Berretta, S., Heckers, S., and Konradi, C. (2011). Bipolar disorder type 1 and schizophrenia are accompanied by decreased density of parvalbumin- and somatostatin-positive interneurons in the parahippocampal region. Acta Neuropathol. *122*, 615–626.

Watanabe, K., Kamiya, D., Nishiyama, A., Katayama, T., Nozaki, S., Kawasaki, H., Watanabe, Y., Mizuseki, K., and Sasai, Y. (2005). Directed differentiation of telencephalic precursors from embryonic stem cells. Nat. Neurosci. *8*, 288–296.

Wataya, T., Ando, S., Muguruma, K., Ikeda, H., Watanabe, K., Eiraku, M., Kawada, M., Takahashi, J., Hashimoto, N., and Sasai, Y. (2008). Minimization of exogenous signals in ES cell culture induces rostral hypothalamic differentiation. Proc. Natl. Acad. Sci. USA *105*, 11796–11801.

Wichterle, H., Garcia-Verdugo, J.M., Herrera, D.G., and Alvarez-Buylla, A. (1999). Young neurons from medial ganglionic eminence disperse in adult and embryonic brain. Nat. Neurosci. *2*, 461–466.

Wichterle, H., Turnbull, D.H., Nery, S., Fishell, G., and Alvarez-Buylla, A. (2001). In utero fate mapping reveals distinct migratory pathways and fates of neurons born in the mammalian basal forebrain. Development *128*, 3759–3771.

Ying, Q.L., Stavridis, M., Griffiths, D., Li, M., and Smith, A. (2003). Conversion of embryonic stem cells into neuroectodermal precursors in adherent monoculture. Nat. Biotechnol. *21*, 183–186.

Zerucha, T., Stuhmer, T., Hatch, G., Park, B.K., Long, Q., Yu, G., Gambarotta, A., Schultz, J.R., Rubenstein, J.L., and Ekker, M. (2000). A highly conserved enhancer in the Dlx5/Dlx6 intergenic region is the site of cross-regulatory interactions between Dlx genes in the embryonic forebrain. J. Neurosci. *20*, 709–721.

Zimmerman, L., Parr, B., Lendahl, U., Cunningham, M., McKay, R., Gavin, B., Mann, J., Vassileva, G., and McMahon, A. (1994). Independent regulatory elements in the nestin gene direct transgene expression to neural stem cells or muscle precursors. Neuron *12*, 11–24.